PERGAMON

International Journal of Heat and Mass Transfer 43 (2000) 2421–2429

International Journal of HEAT and MASS TRANSFER

www.elsevier.com/locate/ijhmt

Technical Note

Non-Darcy mixed convection in a vertical channel filled with a porous medium

Y.C. Chen[a,*], J.N. Chung[b], C.S. Wu[c], Y.F. Lue[c]

[a]*Department of Mechanical Engineering, Oriental Institute of Technology, Panchiao 220, Taiwan, ROC*
[b]*Department of Mechanical Engineering, University of Florida, Gainesville, FL 32611-6300, USA*
[c]*Department of Agriculture Machinery, National Taiwan University, Taipei, Taiwan, ROC*

Received 6 May 1999; received in revised form 23 September 1999

1. Introduction

The fluid flow and heat transfer through a porous medium has been extensively studied in the past, because of its relevance to nuclear waste disposal, solid matrix heat exchanger, thermal insulation and other practical applications. For the laminar wall-bounded forced convection, the heat transfer characteristics have been widely investigated by researchers [1–4]. For the mixed convection flow, Parang and Keyhani [5] studied the fully developed buoyancy-assisted mixed convection in a vertical annulus by using the Brinkman-extended Darcy model. Their results indicated that the Brinkman term could be neglected for lower Darcy number. Muralidhar [6] performed a numerical calculation for buoyancy-assisted mixed convection in a vertical annulus by using the Darcy model. The results show that the Nusselt number increases with the Rayleigh number and/or Peclet number. Hadim and Chen [7] investigated the Darcy number effects on the buoyancy-assisted mixed convection in the entrance region of a vertical channel with asymmetric heating at fixed values of Reynolds number, Forchheimer number, Prandtl number, and modified Grashof number. Their results showed that as the Darcy number is decreased, distortions in the velocity profile lead to increased heat transfer. In this paper the fully developed mixed convection in a vertical porous channel with a uniform heat flux imposed at the plates is investigated by using the Brinkman–Forchheimer-extended Darcy model. Both buoyancy-assisted and buoyancy-opposed flows are considered. The effects of the parameters on the heat transfer characteristics are examined in details.

2. Formulation

The problem under investigation is the fully developed mixed convection between two long vertical plates filled with a fluid-saturated porous medium. The uniform heat flux condition is symmetrically imposed on both walls. The porous medium is assumed to be isotropic and homogenous (with constant porosity and effective thermal diffusivity). The thermophysical properties of solid matrix and fluid are also assumed to be constant except the density variation in the momentum equations. The governing equations for momentum and energy for the up-flow with heated or cooled walls can be written as:

$$-\frac{\mathrm{d}P^*}{\mathrm{d}x^*}-\frac{\mu_\mathrm{f}}{K}U^*-\rho_\mathrm{f}\frac{c_\mathrm{F}}{\sqrt{K}}|U^*|U^*+\rho_\mathrm{f}g\beta\left(T^*-T^*_\mathrm{w}\right)+\mu_\mathrm{e}\frac{\mathrm{d}^2U^*}{\mathrm{d}y^{*2}}=0 \tag{1}$$

$$U^*\frac{\partial T^*}{\partial x^*}=\frac{\partial}{\partial y^*}\left(\alpha_\mathrm{m}\frac{\partial T^*}{\partial y^*}\right) \tag{2}$$

* Corresponding author.

0017-9310/00/$ - see front matter
PII: S0017-9310(99)00299-9

Nomenclature

c_F	form drag constant
Da^*	modified Darcy number, defined in Eq. (7)
F	Forchheimer number, defined in Eq. (7)
g	gravitational acceleration
K	permeability
L	half width of the channel
Nu	Nusselt number, defined in Eq. (3)
P	pressure
Ra	Rayleigh number, defined in Eq. (7)
T^*, T^*_m	temperature and mean temperature
U, U_m	fluid velocity and mean fluid velocity
x, y	streamwise and cross-streamwise coordinates

Greek symbols

α_m	effective thermal diffusivity
β	thermal expansion coefficient
θ	dimensionless temperature, defined in Eq. (4)
μ_e, μ_f	effective viscosity and fluid viscosity
ν_e	effective kinematic viscosity
ρ_f	fluid density

For a constant heat flux at the walls, the wall temperature is assumed to increase linearly with x^* as $T^*_w = T^*_0 + C_1 x^*$, where C_1 is a constant and T^*_0 is the upstream reference temperature. The Boussinesq approximation is used here. The Nusselt number is defined as

$$Nu = 2L\frac{\left.\frac{dT^*}{dy^*}\right|_{y^*=L}}{(T^*_w - T^*_m)} \tag{3}$$

The nondimensionalization is carried out based on the following definition.

$$x = \frac{x^*}{L}, \quad y = \frac{y^*}{L}, \quad P = P^*\frac{L^2}{\rho_f \nu_e^2}, \quad U = \frac{U^*}{\frac{\nu_e}{L}\left(-\frac{dP}{dx}\right)}, \quad \theta = \frac{T^* - T^*_w}{C_1 L\frac{\nu_e}{\alpha_m}\left(-\frac{dP}{dx}\right)} \tag{4}$$

The dimensionless momentum and energy equations with homogenous boundary conditions at walls are

$$1 - \frac{1}{Da^*}U - Fo|U|U + Ra\,\theta + \frac{d^2U}{dy^2} = 0 \tag{5}$$

$$U = \frac{d^2\theta}{dy^2} \tag{6}$$

There are three dimensionless parameters, the modified Darcy number, Da^*, the Forchheimer number, F, and the Rayleigh number, Ra. They are defined as

$$Da^* = \frac{\mu_e}{\mu_f}\frac{K}{L^2}, \quad F = \frac{c_F L}{\sqrt{K}}\left(-\frac{dP}{dx}\right), \quad Ra = \frac{g\beta C_1 L^4}{\nu_e \alpha_m} \tag{7}$$

3. Numerical method

The Galerkin method is used to solve the above coupled equation (5) and (6) and their associated boundary conditions. In this method, the test (weight) functions are the same as the base (trial) functions. Thus U, θ, and the base function, $\xi_n(y)$, are expressed in the following.

$$U = \sum_{n=0}^{N} a_n \xi_n(y), \ \theta = \sum_{n=0}^{N} b_n \xi_n(y), \ \xi_n(y) = (1 - y^2)P_n(y) \tag{8}$$

where a_n and b_n are the unknown coefficients and $P_n(y)$ is the Legendre polynomial of order n. The above method has been used successfully in the stability analysis [8,9]. By substituting Eq. (8) into Eqs. (5) and (6), a set of nonlinear equations is produced. The resulting nonlinear system is solved by the Newton method [10]. The other details can be found in Chen and Chung [9]. Generally, the criterion used for the iteration convergence is

$$\mathrm{Max}\left|\frac{a_n^{i+1} - a_n^i}{a_n^i}\right| \le 10^{-7}, \quad \text{and} \quad \mathrm{Max}\left|\frac{b_n^{i+1} - b_n^i}{b_n^i}\right| \le 10^{-7} \tag{9}$$

where a_n^i and b_n^i are the values at the iteration number i. We first verified our code by comparing with the published results of forced convection ($Ra = 0$). Nield et al. [4] showed that Nu is about 4.52 (estimated from their Fig. 2(b) for $\mu_e/\mu_f = 10$) for $F = 10^2$ and $Da^* = 10$, and the exact solutions of the Nusselt numbers for $F = 0$ and $Da^* = 0.01$ and 10 are 5.129 and 4.122, respectively. Our computed Nusselt numbers with $N = 51$ in Eq. (8) produce the same results. It is

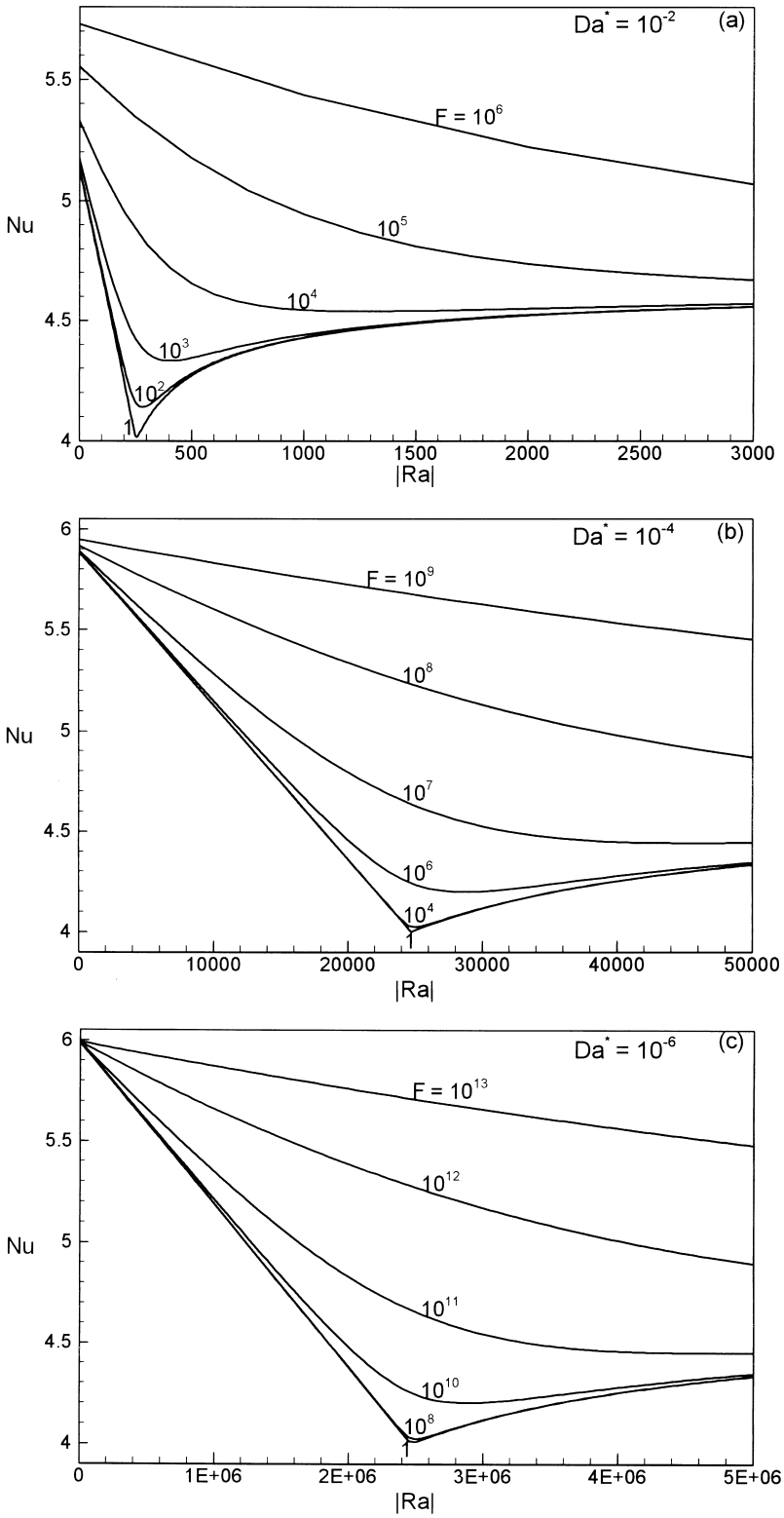

Fig. 1. The variation of the Nusselt number with the Rayleigh number for the buoyancy-assisted flow at (a) $Da^* = 10^{-2}$; (b) $Da^* = 10^{-4}$; and (c) $Da^* = 10^{-6}$.

noted that for $\mu_e/\mu_f = 10$, their Darcy number of 1 and Forchheimer number of 10^4 shown in their Fig. 2(b) are equivalent to the $Da^* = 10$ and $F = 10^2$ in this paper. For a large value of F, our computed Nu is 5.99 for $F = 10^{12}$ and $Da^* = 0.01$, which is approaching to the 'slug flow' value of 6. For the mixed convection, the analytic solution of Nu for $F = 0$ can be derived from Eqs. (5) and (6) and is given in the following for the case of $0 < 4Da^{*2}Ra < 1$.

$$Nu = \frac{-4(a^2 b \tanh b - b^2 a \tanh a)\left[(\tanh a)/a + (\tanh b)/b\right]}{\dfrac{b^2\left[2 + (\sinh 2a)/a\right]}{2\cosh^2 a} - \dfrac{\left(a^2 + b^2\right)}{\cosh a \cosh b}\left[\dfrac{\sinh(a+b)}{a+b} + \dfrac{\sinh(a-b)}{a-b}\right] + \dfrac{a^2\left[2 + (\sinh 2b)/b\right]}{2\cosh^2 a}} \tag{10}$$

where $a = \{[1 + (1 - 4Da^{*2}Ra)^{1/2}]/(2Da^*)\}^{1/2}$ and $b = \{[1 - (1 - 4Da^{*2}Ra)^{1/2}]/(2Da^*)\}^{1/2}$. Our computed Nusselt numbers for $Ra = 1000$ and $Da^* = 10^{-2}$ and $Ra = 5 \times 10^4$ and $Da^* = 10^{-4}$ for $F = 0$ are 8.45 and 9.32, respectively. These agree exactly with the above solutions.

4. Results and discussion

The dimensionless parameters in the system are the modified Darcy number, Da^*, Rayleigh number, Ra, and Forchheimer number, F. The Rayleigh number is positive or negative for the buoyancy-assisted or buoyancy-opposed flows, respectively. In this study, Da^* of 10^{-2}, 10^{-4} and 10^{-6} are chosen for sample calculation. As indicated in Eq. (8), the Forchheimer number is the combination of the form drag term and the pressure gradient (or the Reynolds number), thus we have a wide range to choose its value. In the buoyancy-assisted flow, the variation of the Nusselt number with the Rayleigh number for $Da^* = 10^{-2}$ is plotted in Fig. 1(a) for F ranging from 1 to 10^6. All curves show that the Nusselt number increases with increasing Rayleigh number, but the rate of increase is slower, when the Forchheimer number becomes higher. The Nusselt number at $Ra = 5000$ is 2.5 times than that of the pure forced convection ($Ra = 0$) for $F \leq 10^4$. This indicates that the buoyancy force has an important effect on the Nusselt number for lower F. The maximum deviation of Nu for $F = 10^3$ and $F = 10^4$ from that of $F = 1$ is about 2% and 6.3%, respectively. This implies that the Forchheimer number has a very minor effect on the Nusselt number for $F \leq 10^3$. Fig. 1(a) also shows the different effects of the Forchheimer number on Nu for forced convection and mixed convection. The Nusselt number increases very slowly with increasing Forchheimer number for the pure forced convection ($Ra = 0$), while Nu decreases quickly with the increase of Forchheimer number for mixed convection dominated regime. Fig. 1(b) plots the results for $Da^* = 10^{-4}$. It shows that the modified Darcy number has an important effect on the Nusselt number. The Nusselt number at $Ra = 4000$ for $Da^* = 10^{-2}$ and $F = 1$ is 13.14 while its corresponding Rayleigh number for $Da^* = 10^{-4}$ and $F = 1$ for the same Nu is as high as about 1.55×10^7, which is 35 times larger than that for $Da^* = 10^{-2}$. This figure also shows that Nu increases with increasing Rayleigh number. As shown in Fig. 3(a), this is because the buoyancy force significantly increases the fluid velocities near the wall regions, when Ra is higher. The curves for $F = 1$ and 10^6 are almost overlapping with each other. The maximum deviation of Nu between $F = 1$ and 10^7 is 3% in Fig. 1(a). This indicates that the Forchheimer number effect is negligible for $F \leq 10^7$. The variation of Nu for $F \geq 10^8$ from that of $F = 1$ becomes significant. At $Ra = 2 \times 10^5$, the variation in Nu between $F = 10^7$ and 10^8 is 2.33, while it is as high as 4.18 between $F = 10^8$ and 10^9. The decreasing rate of Nu is reduced for $F \geq 10^9$. The variation of the Nusselt number with the Rayleigh number for $Da^* = 10^{-6}$ is shown in Fig. 1(c). In general, the behaviors of the curves follow the similar trends for $Da^* = 10^{-4}$. It again shows that the modified Darcy number has an important effect on the Nusselt number. The Nusselt number for $Da^* = 10^{-4}$ and $F = 1$ at $Ra = 1.8 \times 10^5$ is 15.73, while for $Da^* = 10^{-6}$ and $F = 1$, the Rayleigh number for the same Nusselt number is as high as about 1.55×10^7, which is about 86 times larger than that of $Da^* = 10^{-4}$. The maximum deviation of Nu between $F = 1$ and 10^{11} in Fig. 1(c) is 3.8%. From those results in Fig. 1(a)–(c), it may be concluded that the Forchheimer number effect on the Nusselt number is negligible for $F \leq 0.1/Da^{*2}$.

For the buoyancy-opposed flow, Fig. 2(a) plots the variation of the Nusselt number with the Rayleigh number for $Da^* = 10^{-2}$. It shows that Nus for all curves are smaller than that of the pure forced convection ($Ra = 0$). In the beginning, Nus for all curves decrease with the increasing of the absolute value of Rayleigh number $|Ra|$ until $|Ra|$ reaches a threshold value. At this threshold value of $|Ra_t|$, the Nusselt number is the minimum. It can be seen that Nus for $F = 1$ and 100 decrease very quickly and they are close to a straight line for $|Ra|$ lesser

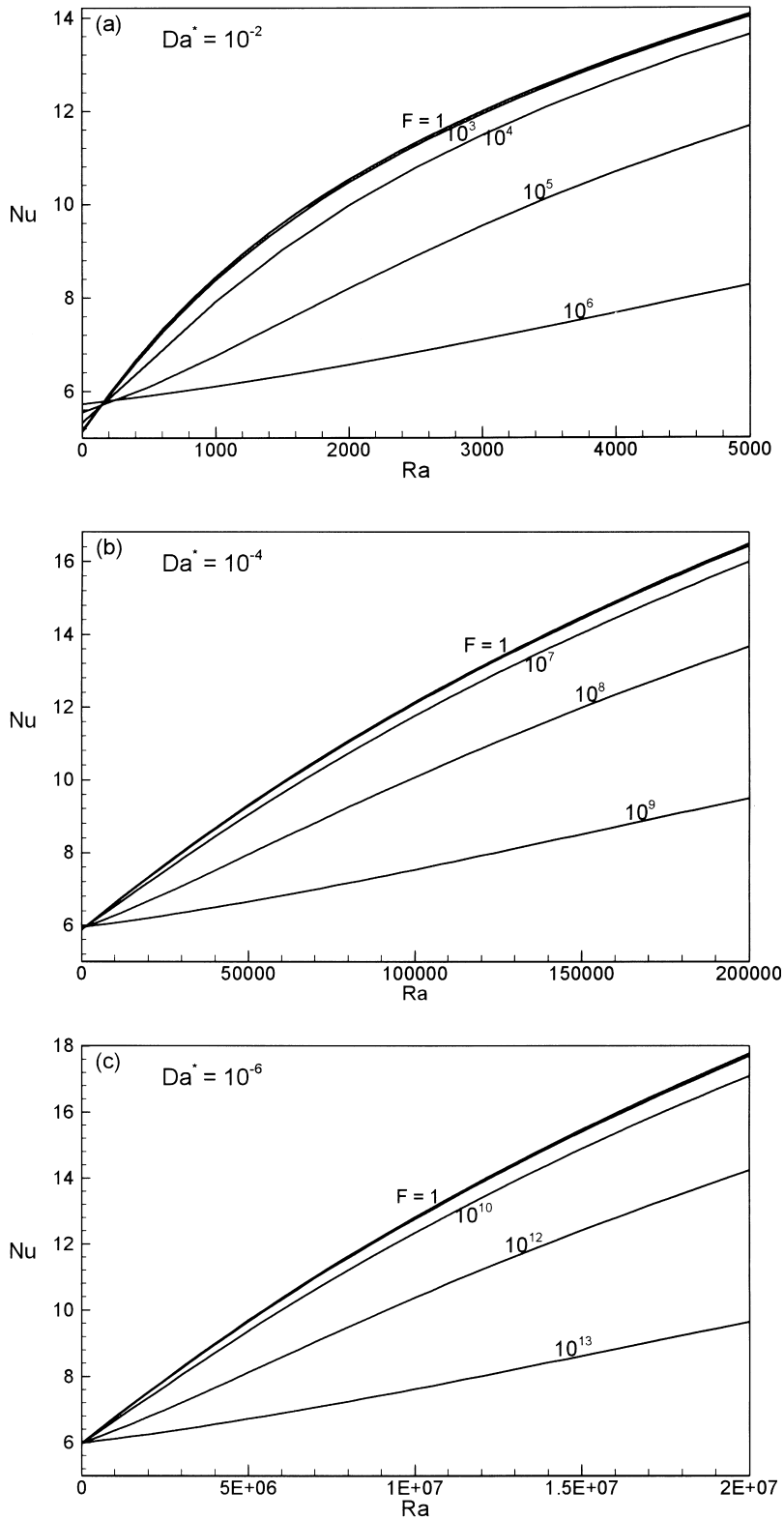

Fig. 2. The variation of the Nusselt number with the Rayleigh number $|Ra|$ for the buoyancy-opposed flow at (a) $Da^* = 10^{-2}$, (b) $Da^* = 10^{-4}$, and (c) $Da^* = 10^{-6}$.

than about 250, while for $F = 10^6$, Nu decreases slowly, that is, the decreasing speed is slower; when F is higher. Then $|Ra|$ is greater than $|Ra_t|$, Nu increases with increasing $|Ra|$. These threshold values of $|Ra_t|$ for $F = 1$, 10^2, 10^3, 10^4, 10^5 and 10^6 are about 255, 290, 400, 1300, 7700 and 50000, respectively. This indicates that the threshold value of $|Ra_t|$ increases with increasing F and it changes only slightly for $F \leq 10^3$, while it increases quickly for $F \geq 10^4$. The Nusselt number for lower Forchheimer number ($F = 1$ and 100) increases more quickly than the other cases in the beginning after $|Ra|$ is greater than $|Ra_t|$. When the Forchheimer number is higher, the rate of increase for Nu is slower when $|Ra|$ is greater than $|Ra_t|$ and then the rate of increase is gradually reduced with increasing $|Ra|$. The variation of the Nusselt number

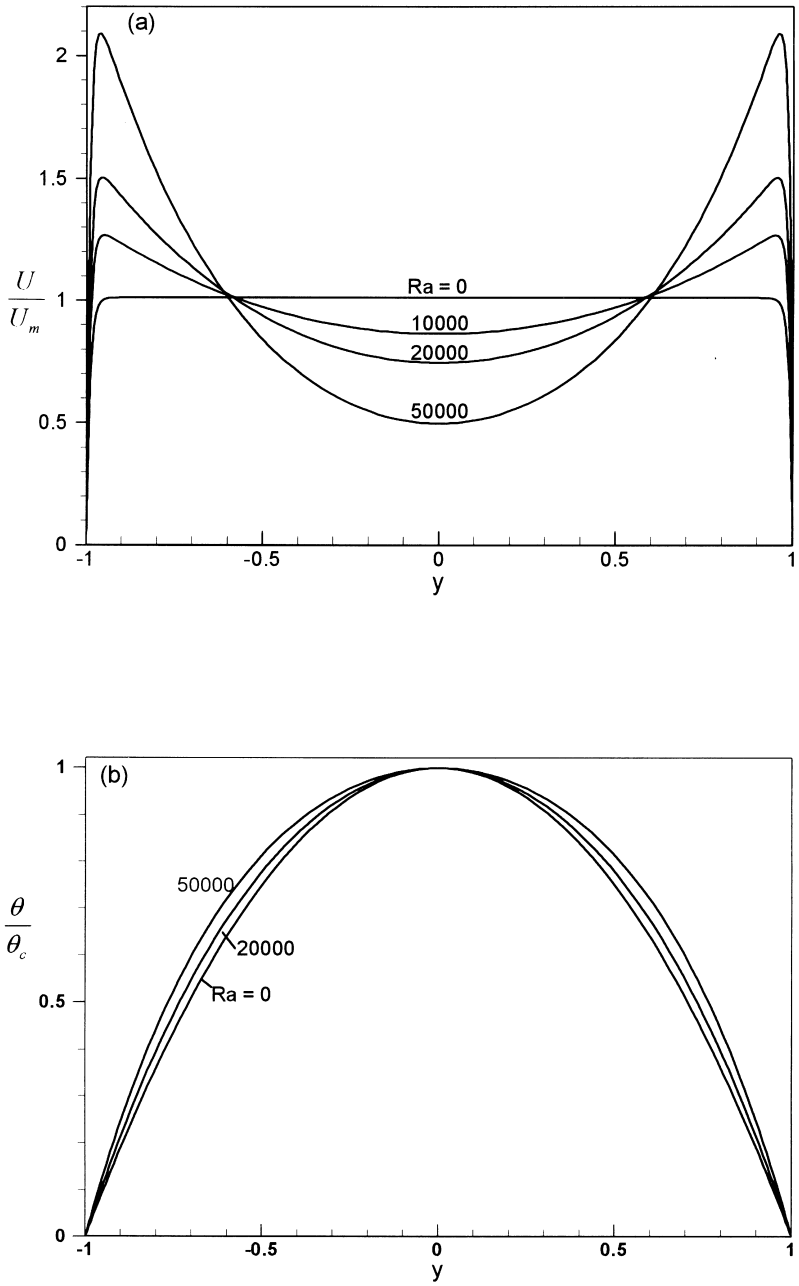

Fig. 3. The (a) velocity and (b) temperature profiles at various Rayleigh numbers for the buoyancy-assisted flow at $Da^* = 10^{-4}$ and $F = 1$.

with the Rayleigh number for $Da^* = 10^{-4}$ is plotted in Fig. 2(b). It shows that the modified Darcy number has an important effect on the Nusselt number. For $|Ra|$ smaller than the threshold value, Nu at $|Ra| = 245$ for $Da^* = 10^{-2}$ and $F = 1$ is 4.04, while its corresponding Ra for the same Nu for $Da^* = 10^{-4}$ and $F = 1$ is as high as about 24,000, which is about 98 times larger than that for $Da^* = 10^{-2}$. For $|Ra| < |Ra_t|$, Nu also decreases with increasing $|Ra|$, and the decreasing speed is slower when F is higher. These threshold

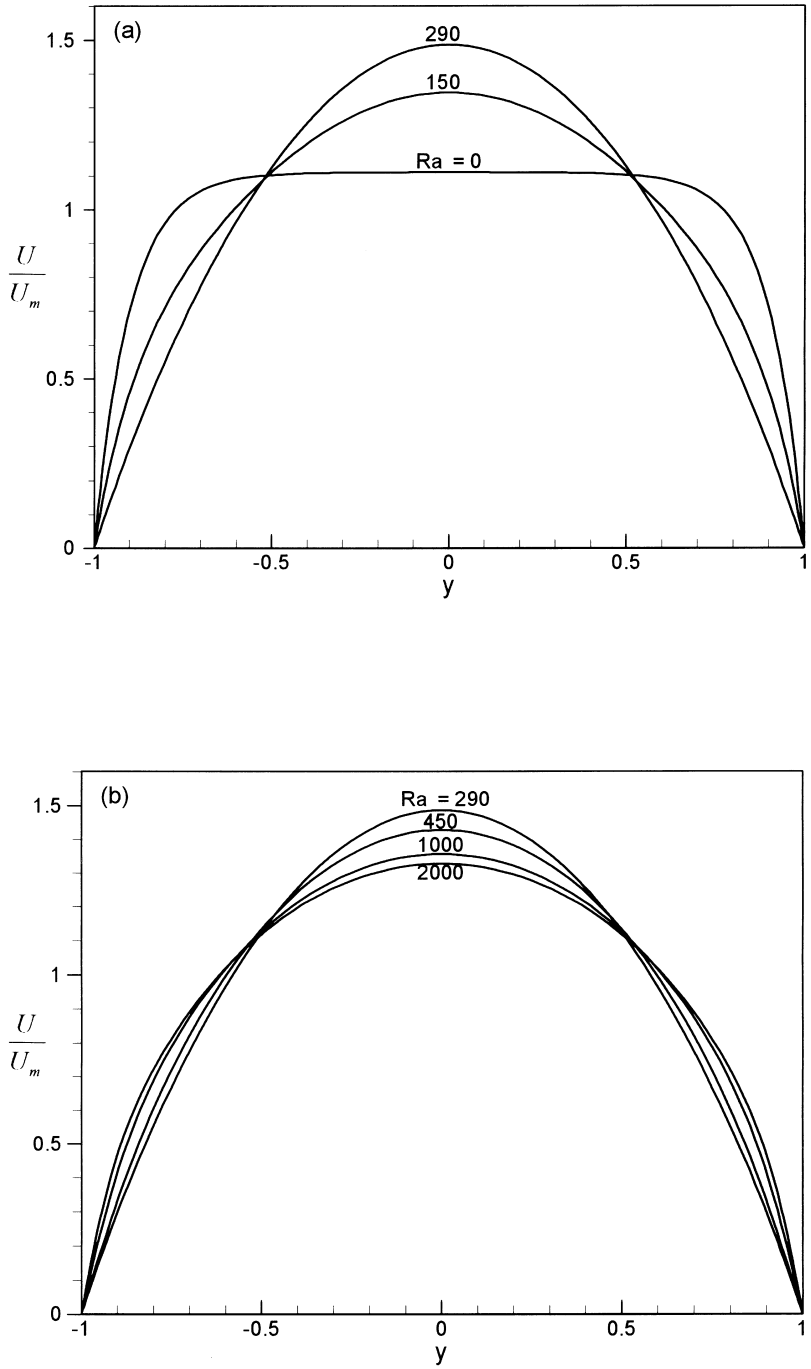

Fig. 4. The velocity profiles for the buoyancy-opposed flow at $Da^* = 10^{-2}$ and $F = 10^2$ for (a)$|Ra| \leq |Ra_t|$ and (b)$|Ra| \geq |Ra_t|$.

values of $|Ra_t|$ for $F = 1$, 10^4, 10^6, 10^7 and 10^8 are about 24,700, 25,000, 29,000, 47,000 and 200,000, respectively. The threshold value of $|Ra_t|$ for $Da^* = 10^{-2}$ and $F = 1$ is about 255, while it is as high as about 24,700 for $Da^* = 10^{-4}$ and $F = 1$. This also indicates that the modified Darcy number significantly affects the threshold value of $|Ra_t|$. The threshold value of $|Ra_t|$ also changes slightly for $|Ra| \leq 10^6$. The maximum deviation of Nu between $F = 1$ and 10^6 is about 5%. This implies that the Forchheimer number effect on the Nusselt number is negligible for $F \leq 10^6$. Fig. 2(c) plots the results for $Da^* = 10^{-6}$. It again shows that the modified Darcy number has an important effect on the Nusselt number. The $|Ra_t|$ for $Da^* = 10^{-4}$ and $F = 1$ is about 2.43×10^4, while it is about 2.43×10^6 for $Da^* = 10^{-6}$ and $F = 1$, which is about 100 times larger than that for $Da^* = 10^{-4}$. For $|Ra| < |Ra_t|$, Nu decays with increasing $|Ra|$ and the decaying speed is slower for higher F. The maximum deviation of Nu between $F = 1$ and 10^{10} is about 5.9%. From the above results in Fig. 2(a)–(c), it may be concluded that the Forchheimer number effect on Nu is minor for $F \leq 0.01/Da^{*2}$.

The velocity profile (U/U_m) and temperature profile (θ/θ_c) for the buoyancy-assisted flow at $Da^* = 10^{-4}$ are plotted in Fig. 3(a) and (b), respectively, where θ_c is the temperature at the center of the channel. For the pure forced convection ($Ra = 0$), the velocity profile is almost a flattened straight line except at very near wall regions. When the Rayleigh number increases, the buoyancy force acts to increase the fluid velocity in the near wall region. The velocity increase in the very near wall region will enhance the convection heat transfer and thus increase the Nusselt number. The increase of fluid velocity in the very near wall region will result in a decrease of fluid velocity at the center region of the channel. When Ra is high, the maximum velocity in the near wall region is significantly higher than the fluid velocity at the center of the channel. As shown in Fig. 3(b), the temperature profile becomes more flattened, when Ra increases, this indicates that the mean temperature is higher for higher Ra. Fig. 4(a) and (b) show the velocity profiles (U/U_m) for the buoyancy-opposed flow at $Da^* = 10^{-2}$ and $F = 100$ with $|Ra| \leq |Ra_t|$ and $|Ra| \geq |Ra_t|$, respectively. It is noted that the threshold value of $|Ra_t|$ for $Da^* = 10^{-2}$ and $F = 100$ is about 290. Fig. 4(a) shows that when $|Ra|$ increases, since the buoyancy force acts to decrease the fluid velocity in the near wall region and as a consequence, lower the convection heat transfer and then decrease the Nusselt number. The decrease of fluid velocity in the near wall region will result in an increase of fluid velocity at the center regions of the channel. When the value of $|Ra|$ is greater than the threshold value, as shown in Fig. 4(b), the fluid velocity in the near wall region slowly increases with the increase of $|Ra|$, but it is always smaller than the fluid velocity in the wall region for the pure forced convection. Thus Nu for the buoyancy-opposed mixed convection is always smaller than that of forced convection. The fully developed mixed convection flow may be unstable under approximate conditions. This topic is currently under investigation [11].

5. Conclusions

The numerical calculation of the fully developed mixed convection in a heated vertical channel filled with a porous medium with imposed uniform heat flux at the plates was performed using the Brinkman–Forchheimer-extended Darcy model. The Galerkin method was employed in this calculation. Both the buoyancy-assisted and buoyancy-opposed flows are considered. The effects on the heat transfer characteristics from all the related parameters, the modified Darcy number, Da^*, the Forchheimer number, F, and the Rayleigh number, Ra, are also examined. It is shown that the buoyancy force can significantly affect the Nusselt number for higher Rayleigh numbers, higher modified Darcy numbers and/or lower Forchheimer numbers. The modified Darcy number has an important effect on the Nusselt number. For the buoyancy-assisted flow, the buoyancy force acts to increase the fluid velocity for the near wall region and then increases Nu when Ra is increased. The rate of increase in Nu is higher, when Da^* is higher and/or F is lower. It also shows that the Forchheimer number effect on Nu is negligible for $F \leq 0.1/Da^{*2}$. For the buoyancy-opposed flow, the buoyancy force acts to decrease the fluid velocity for the near wall region. In the beginning, Nu decreases quickly with the increasing $|Ra|$ before the $|Ra|$ reaches a threshold value, $|Ra_t|$. After this threshold value, Nu increases slowly with increasing $|Ra|$, but it is always smaller than that of the pure forced convection. The value of $|Ra_t|$ strongly depends on the modified Darcy number and Forchheimer number. It is higher when Da^* is smaller and/or F is larger. The Forchheimer number effect on Nu is minor for $F \leq 0.01/Da^{*2}$.

Acknowledgements

This research work was supported by National Science Council, R.O.C., under grant NSC 87-2621-B-161-001.

References

[1] K. Kaviany, Laminar flow through a porous channel bounded by isothermal parallel plates, Int. J. Heat Mass Transfer 28 (1985) 851–858.

[2] P. Cheng, C.T. Hsu, Fully-developed, forced convective flow through an annular packed-sphere bed with wall effects, Int. J. Heat Mass Transfer 29 (1986) 1843–1853.

[3] K. Vafai, S.J. Kim, Forced convection in a channel with a porous medium: an exact solution, ASME J. Heat Transfer 111 (1989) 1103–1106.

[4] D.A. Nield, S.L.M. Junqueira, J.L. Large, Forced convection in a fluid-saturated porous-medium channel with isothermal or isoflux boundaries, J. Fluid Mech 322 (1996) 201–214.

[5] M. Parang, M. Keyhani, Boundary effects in laminar mixed convection flow through an annular porous medium, ASME J. Heat Transfer 109 (1987) 1039–1041.

[6] M. Muralidhar, Mixed convection flow in a saturated porous annulus, Int. J. Heat Mass Transfer 32 (1989) 881–888.

[7] A. Hadim, G. Chen, Non-Darcy mixed convection in a vertical porous channel, J. Thermophysics and Heat Transfer 8 (1994) 805–808.

[8] Y.C. Chen, J.N. Chung, The linear stability of mixed convection in a vertical channel flow, J. Fluid Mech 325 (1996) 29–51.

[9] Y.C. Chen, J.N. Chung, Stability of mixed convection in a differentially heated vertical channel, ASME J. Heat Transfer 120 (1998) 127–132.

[10] R.L. Burden, J.D. Faires, Numerical Analysis, PWS-KENT, Boston, MA, 1988.

[11] Y.C. Chen, J.N. Chung, Non-Darcy flow stability of mixed convection in a vertical channel filled with a porous medium (1999) (to be submitted).